What Influences Barrier Heights in Hydrogen Abstraction from Thiols by Carbon-Centered Radicals? A Curve-Crossing Study

Kaitlin D. Beare and Michelle L. Coote*

Research School of Chemistry, Australian National University, Canberra, ACT 0200, Australia

Received: May 4, 2004; In Final Form: June 28, 2004

High-level ab initio molecular orbital calculations have been used to study the barriers and enthalpies for hydrogen atom abstraction reactions of the form RS−H + •R′ → RS• + H−R′ for combinations of R, R′ = CH_3, CH_2Cl, $CHCl_2$, CCl_3 CH_2F, CH_2OH, CH_2SH, CH_2CN, CH_2CH_3, $CH_2CH_2CH_3$, CH_2Ph, and $CH_2C(CH_3)_3$. The results are analyzed with the aid of the curve-crossing model. Hydrogen abstraction by carbon-centered radicals from thiols is generally an exothermic process in which a strong C−H bond is formed at the expense of the weaker S−H bond of the thiol. However, the exothermicities are strongly influenced by substituents on the attacking radical (and, to a lesser extent, the thiol), and the reverse reaction could be thermodynamically preferred for appropriately substituted systems. The barrier heights are predominantly influenced by polar factors, with the reactions of nucleophilic radicals (such as $•CH_2OH$) being favored over reactions with electrophilic radicals (such as $•CH_2CN$). However, other factors, such as the reaction exothermicity, the strength of the forming and breaking bonds, and (in some cases) direct H-bonding interactions in the transition structures, also contribute to the trends in the barriers.

1. Introduction

Hydrogen abstraction is one of the most fundamental reactions of free radicals, featuring in applications as diverse as combustion, polymerization, atmospheric chemistry, interstellar chemistry, and biochemistry. An important class of these reactions is hydrogen atom abstraction from thiols by carbon-centered radicals:

$$RS{-}H + {}^{\bullet}R' \rightarrow RS^{\bullet} + H{-}R' \qquad (1)$$

This process is important in free-radical polymerization, where thiols are often used as chain transfer agents to limit the molecular weight of the resulting polymer.[1] The reaction also features in organic synthesis, where it forms the first step of an organotin-free catalytic reduction process.[2] Moreover, in the biological field, the reaction of thiols with polypeptide radicals is generally regarded as an important repair mechanism for limiting oxidative damage in proteins.[3] An understanding of the factors influencing radical reactivity in these reactions is important, as this can aid in the design of improved methods for modeling and controlling these reactions.

Hydrogen abstraction reactions have long been the focus of efforts to model and interpret trends in reactivity via theoretical,[4−16] group additivity,[17,18] and empirical[19−23] approaches. Despite this attention, the factors influencing reactivity in these reactions remain the topic of considerable debate. For example, some theoretical studies have indicated that the barrier height in the reaction $X^{\bullet} + H{-}Y \rightarrow X{-}H + {}^{\bullet}Y$ is primarily influenced by the reaction exothermicity and the *short-range* triplet repulsive interactions in the forming and breaking X−H and Y−H bonds.[8−12,14,15] This latter interaction has in turn been modeled by using the singlet−triplet gap of the closed-shell Y−H and X−H substrates,[8−10,12] or the corresponding X−H and Y−H bond dissociation energies,[9,10,15] or the "intrinsic barriers" (as defined in Marcus theory[24]) for the corresponding identity reactions.[8,10,14] In contrast, other studies have concluded that the *long-range* triplet repulsive interactions, involving unpaired electrons on the centers between which the hydrogen is transferred, are also important, and hence the reaction barrier also depends on the properties of the X−Y bond.[4−7] Both theories have thus far been able to account for the effects of substituents in the majority of hydrogen atom abstraction reactions, though the physical validity of the alternative models has been a point of contention.[9]

The role of polar effects in hydrogen abstraction reactions has also been the topic of some debate. For example, Pross et al.[8] concluded that polar effects were not important in determining the trends in the barriers for the reaction of alkyl radicals with hydrogen atoms, but were important for the corresponding reactions with chlorine atoms. Polar effects have also been reported by Fox and Schlegel[14] for the reactions of $•CH_2CN$ with CH_3OH and CH_3NH_2, and by Salikhov and Fischer[12] for model three-electron systems. More generally, the empirical scheme of Roberts and Steel,[19] which has been successfully fitted to the reaction barriers of a wide range of abstraction reactions, includes a specific contribution from polar interactions, measured as the difference in the Pauling electronegativity parameters for the reactants. In contrast to this work, Song et al.[10] recently noted that, for the nonidentity reactions involving transfer between combinations of $•CH_3$, $•SiCH_3$, $•GeH_3$, $•SnH_3$, and $•PbH_3$ radicals, there was a significant contribution of the ionic resonance structures in the transition structure. However, these polar interactions were not contributing to the *trends* in the reaction barriers, because the covalent-ionic resonance energy was relatively constant within the series—despite the differences in the electronegativities of the various radicals.

* To whom correspondence should be addressed. E-mail: mcoote@rsc.anu.edu.au.

10.1021/jp048092s CCC: $27.50
Published on Web 08/06/2004

There have also been mixed results concerning the role of polar effects in hydrogen atom abstraction from thiols by carbon-centered radicals. For example, Zavitsas and Chatgilialoglu[6] argued that polar effects are not important in reactions of methyl radicals with thiols, on the basis of the small electronegativity difference between sulfur and carbon. However, in response, Roberts[19c] argued that, while not important for the reaction of $CH_3^\bullet$ with CH_3SH, the polar effect would be predicted to become more important for reactions with more nucleophilic radicals. Indeed, experimental studies have indicated that the reactivity of thiols is strongly influenced by the electronegativity of the attacking radical.[2,25−28] More recently, Reid et al.[29,30] examined hydrogen abstraction from thiols by hydroxyradicals, and also hydrogen abstraction from peptides by thiyl radicals, and observed a large influence of polar interactions in these reactions. It thus seems clear that polar effects do play a role in certain hydrogen abstraction reactions, but their general importance is yet to be clearly established. Understanding the role of polar effects in hydrogen abstraction from thiols will contribute to a better understanding of the effects of the solvent on such reactions, and will assist in improving synthetic procedures (such as polarity reversal catalysis[2]).

The aim of the present work is to provide a more general understanding of the factors influencing barrier heights in hydrogen abstraction from thiols by carbon-centered radicals. To this end, barriers and enthalpies have been calculated for reaction 1 for a wide range of both polar and nonpolar substituents (R, R′ = CH_3, CH_2Cl, $CHCl_2$, CCl_3 CH_2F, CH_2OH, CH_2SH, CH_2CN, CH_2CH_3, $CH_2CH_2CH_3$, CH_2Ph, $CH_2C(CH_3)_3$), on both the carbon-centered radical and the thiol. To provide a theoretical framework for rationalizing the results we make use of the curve-crossing model.[31−33] This model has recently been used to study other types of hydrogen abstraction reactions,[8−10,12] as well as other radical reactions, such as radical addition to C═C bonds,[34] and to other types of multiple bonds.[35−37] A more complete description of the model can be found in these previous studies, but the main features are outlined briefly below.

2. Curve-Crossing Model

The curve-crossing model[31−33] (also known as the valence-bond state correlation model, the configuration mixing model, or the state correlation diagram) was developed by Pross and Shaik[31−33] as a unifying theoretical framework for explaining barrier formation in chemical reactions. It is largely based on valence bond (VB) theory,[38] but also incorporates insights from qualitative molecular orbital theory.[39] In broad terms, it seeks to build the energy profile for a chemical reaction in terms of the resonance interactions between the principal VB configurations of the reacting species. In the case of hydrogen abstraction, the principal VB configurations would be:[9,10]

$$\underset{\text{DA}}{X^\bullet H-Y} \leftrightarrow \underset{DA^3}{X-H\ ^\bullet Y} \leftrightarrow \underset{D^+A^-}{X^+\ H^\bullet\ Y^-} \leftrightarrow \underset{D^-A^+}{X^-\ H^\bullet\ Y^+} \qquad (2)$$

The first configuration (DA) corresponds to the arrangement of electrons in the reactants, the second to that of the products (DA^3), and the latter two (D^+A^- and D^-A^+) to possible charge-transfer configurations. Additional ionic configurations (such as $X^-\ H^+\ Y^\bullet$ and $X^+\ H^-\ Y^\bullet$) can also be written, but these are resonance contributors to reactant or product configurations, and can thus be omitted from a compact state correlation diagram.[9] It should be noted that the configurations shown in (2) were previously[9,10] defined for abstraction reactions involving combinations of X, Y = C, Si, Ge, Sn, and Pb; however, it is a simple extension to apply them to the present system (i.e. X = C and Y = S), as follows:

$$\underset{\text{DA}}{C^\bullet H-S} \leftrightarrow \underset{DA^3}{C-H\ ^\bullet S} \leftrightarrow \underset{D^+A^-}{C^+\ H^\bullet\ S^-} \leftrightarrow \underset{D^-A^+}{C^-\ H^\bullet\ S^+} \qquad (3)$$

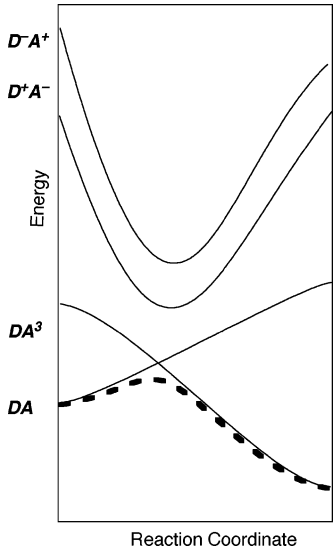

Figure 1. State correlation diagram for hydrogen abstraction from thiols by carbon-centered radicals. The reactant (DA), product (DA^3), and charge-transfer (D^+A^- and D^-A^+) configurations are as shown in eq 3.

The state correlation diagram showing (qualitatively) how the energies of these configurations should vary as a function of the reaction coordinate is provided in Figure 1. In plotting this figure we have arbitrarily designated the D^+A^- configuration to be lower in energy than the D^-A^+ configuration, but it is conceivable that the D^-A^+ could be lower in energy for specific combinations of substituents on the alkyl radical and the thiol. In the early stages of the reaction, the reactant configuration (DA) is the lowest energy configuration and dominates the reaction profile. This is due to the stabilizing influence of the bonding interaction in the H−S bond of the DA configuration, which is an antibonding interaction in the DA^3 configuration. However, as the reaction proceeds, the H−S bond is stretched and the C−H distance decreases. This destabilizes the H−S bond in the DA configuration but stabilizes the DA^3 configuration due to the increasing bonding interaction in the forming C−H bond (which is an antibonding interaction in the DA configuration). As the relative energies of the DA and DA^3 configurations converge, the increasing interaction between the alternative configurations stabilizes the ground state wave function, with the strength of the stabilizing interaction decreasing with the energy difference between the alternate configurations. It is this mixing of the reactant and product configurations that leads to the avoided crossing, and accounts for barrier formation. Beyond the transition structure, the product configuration is lower in energy and dominates the wave function. The charge-transfer configurations of the isolated reactants and the isolated products are high in energy, but in the vicinity of the transition structure they are stabilized via favorable Coulombic interactions and can sometimes be sufficiently low in energy to interact with the ground-state wave function. In those cases, the transition structure is further stabilized, and (if one of the charge-transfer configurations is lower than the other) the mixing is reflected in a degree of partial charge transfer between the reactants.

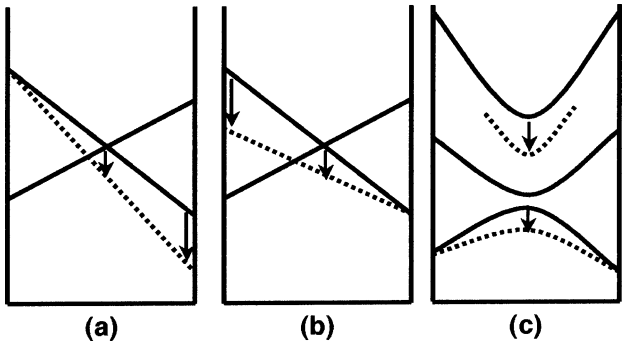

Figure 2. State correlation diagrams showing separately the qualitative effects of (a) increasing the reaction exothermicity, (b) decreasing the singlet−triplet gap, and (c) decreasing the energy of the charge-transfer configuration. For the sake of clarity the adiabatic minimum energy path showing the avoided crossing, as in Figure 1, is omitted from panels a and b.

By using this state-correlation diagram, in conjunction with simple VB arguments, the curve-crossing model can be used to predict the qualitative influence of various energy parameters on the reaction barrier.[31−33] In particular, the barrier is lowered by the following: an increase in the reaction exothermicity (see Figure 2a), and/or a decrease in the DA−DA^3 separation in the reactants and/or products (Figure 2b), and/or a decrease in the relative energies of one or both of the charge-transfer configurations, provided that these are sufficiently low in energy to contribute to the ground-state wave function (Figure 2c). Of these parameters, the reaction exothermicity is of course directly accessible from ab initio molecular orbital calculations. For the hydrogen abstraction reactions, the DA−DA^3 separation is related to the singlet−triplet excitation gap of the closed shell species (i.e. the thiol at the reactant geometry and the alkane at the product geometry).[9,10] It is also related to the bond dissociation energy of the breaking and forming bonds.[9,10] It should be noted that, in studies of radical addition reactions, the DA−DA^3 separation at the reactants only is used to model the barrier height,[34−37] and this is justifiable in terms of the early transition structures in these reactions. In hydrogen abstractions, however, the transition structure generally has more product-like character, and it has been shown that the barrier height is related to the average of the reactant and product DA−DA^3 promotion gaps.[10]

The relative energies of the charge-transfer configurations at the transition structure are somewhat more difficult to model in terms of the properties of the isolated reactants or products. In radical addition reactions,[34−37] the energies for charge transfer between the isolated reactants are frequently used to model the corresponding energies at the transition structures, and this can be justified in terms of the early transition structures in these reactions. In the case of the present abstraction reactions, this would entail using the energy for the $C^+\cdots(H-S)^-$ configuration at infinite separation, to model the C^+ $H^\bullet$ S^- configuration at the transition structure. However, since the $H^\bullet$ atom is close to and almost midway between both the S and C centers at the transition structure, one might equally well have chosen the product configuration, $(C-H)^+\cdots S^-$, instead. In fact, neither configuration is particularly appropriate as, by assigning the charge to the whole thiol (or to the whole alkane), one implicitly includes contributions from configurations such as C^+ H^- $S^\bullet$ (in the thiol case) or $C^\bullet$ H^+ S^- (in the alkane case). As noted above, these configurations are resonance contributors to the product and reactant configurations, rather than the (excited) charge-transfer configurations. For these reasons, in the present work we have opted to model the relative energies of the C^+ $H^\bullet$ S^- and C^- $H^\bullet$ S^+ configurations at the transition structure using the charge-transfer energies between the isolated alkyl and thiyl fragments. Thus, for example, the C^+ $H^\bullet$ S^- configuration is modeled as the difference of the (vertical) ionization energy of the alkyl radical and (vertical) electron affinity of the thiyl radical. This effectively considers the three fragments of the configuration C^+ $H^\bullet$ S^- at infinite separation (i.e. $C^+\cdots H^\bullet\cdots S^-$ is calculated relative to $C^\bullet\cdots H^\bullet\cdots S^\bullet$). Of course, this (and any other approximation based on the isolated reactants and/or products) provides a somewhat crude model of the importance of the charge-transfer configurations at the transition structure. Hence, as a secondary test of their importance in these reactions, we also directly examine the charges on these fragments at the transition state geometry.

3. Theoretical Procedures

Barriers and enthalpies for the hydrogen abstraction reactions were obtained with use of standard ab initio molecular orbital theory[40] and density functional theory[41] calculations, carried out with the GAUSSIAN 98,[42] GAUSSIAN 03,[43] and MOLPRO 2000.6[44] programs. Calculations were performed at a high level of theory, which was chosen on the basis of our recent assessment study for hydrogen abstraction reactions involving carbon-centered radicals.[45] Geometries of the reactants, products, and transition structures were optimized at the MPW1K/6-31+G(d,p) level of theory, and zero-point vibrational energy (scaled by a factor of 0.9515)[46] was also calculated at this level. To ensure that the geometries were global (rather than merely local) minimum energy structures, alternative conformations of the reactants, products, and transition structures were first screened at the B3-LYP/6-31G(2df,p) level of theory. Having obtained the MPW1K/6-31+G(d,p) optimized geometries, improved energies were then calculated at the G3X(MP2)-RAD level of theory.[47] This is a high-level composite procedure that approximates coupled cluster energies [URCCSD(T)] with a large triple-ζ basis set, using additivity approximations.

To assist in the qualitative rationalization of the results, the vertical singlet−triplet gaps of the closed shell reactants (i.e. RS−H) and products (i.e. H−R′), and the vertical ionization energies (IEs) and electron affinities (EAs) of the alkyl and thiyl radicals were also calculated. So that all of the calculations could be performed at a consistent level of theory, we adopted a modified G3X(MP2)-RAD method, in which the URCCSD(T)/6-31G(d) and ROMP2/6-31G(d) calculations are replaced with calculations using the 6-31+G(d) basis set. The extra diffuse functions in this modified method, which we refer to as G3X(MP2)-RAD(+), allow for a better description of the anionic species in EA calculations. To help establish the importance of charge-transfer configurations in the transition structures, we also examined the natural bond orbital (NBO) charges on the reacting fragments. These were calculated with use of the MPW1K/6-311+G(3df,2p) wave function, using the structures optimized at the MPW1K/6-31+G(d,p) level of theory.

To identify the factors influencing the barrier heights in these reactions, correlation coefficients between the barrier height (y) and various individual quantities, such as the enthalpy, average singlet−triplet gap of substrates, or the energy for charge transfer between the isolated alkyl and thiyl fragments (x), were calculated via the following standard statistical formula.[48]

$$r = \frac{\sum(x_i - \bar{x})(y_i - \bar{y})}{\sqrt{(\sum(x_i - \bar{x})^2)(\sum(y_i - \bar{y})^2)}} \qquad (4)$$

TABLE 1: Forward Barrier ($\Delta H^{\ddagger}_{fwd}$), Reverse Barrier ($\Delta H^{\ddagger}_{rev}$), Enthalpy ($\Delta H$), Charge-Transfer Energies (R'^{+} SR^{-} and R'^{-} SR^{+}), and NBO Charges (Q) on the Alkyl and Thiyl Fragments in the Transition Structures for $^{\bullet}CH_3 + H-SR \rightarrow CH_3-H + {}^{\bullet}SR$[a]

H−SR	TS[b]	$\Delta H^{\ddagger}_{fwd}$	$\Delta H^{\ddagger}_{rev}$	ΔH	R'^{+} SR^{-}	R'^{-} SR^{+}	Q(alkyl)	Q(thiyl)
H−SCH_3	*1*	17.2	90.1	−72.8	7.97	10.69	0.008	−0.123
H−$SCCl_3$	*2*	5.7	72.2	−66.5	6.67	10.95	0.045	−0.170
H−$SCHCl_2$	*3*	6.9	73.0	−66.0	6.91	10.93	0.043	−0.168
H−SCH_2Cl	*4*	11.4	81.6	−70.2	7.32	10.95	0.027	−0.146
H−SCH_2F	*5*	13.2	86.7	−73.5	7.53	11.22	0.023	−0.141
H−SCH_2(OH)	*6*	13.1	83.8	−70.7	7.63	−	0.020	−0.140
H−SCH_2(SH)	*7*	12.6	84.8	−72.2	7.64	9.42	0.023	−0.142
H−SCH_2(CN)	*8*	9.9	77.2	−67.3	7.09	11.45	0.037	−0.158
H−$SCH_2(CH_3)$	*9*	16.0	87.5	−71.5	7.88	10.50	0.006	−0.119
H−$SCH_2(CF_3)$	*10*	12.1	76.5	−64.4	7.32	11.39	0.028	−0.150
H−SCH_2(Et)	*11*	15.9	87.2	−71.3	7.87	10.43	0.005	−0.119
H−SCH_2(Ph)	*12*	11.8	81.1	−69.3	7.65	9.02	0.017	−0.135
H−SCH_2(*t*-Bu)	*13*	14.0	81.5	−67.5	7.75	10.32	0.009	−0.127

[a] Barriers and enthalpies (0 K, kJ mol^{-1}) were calculated at the G3X(MP2)-RAD level of theory and include MPW1K/6-31+G(d,p) scaled zero-point vibrational energy. Charge-transfer energies (eV) were calculated as the difference in the vertical ionization energy of the donor species and the vertical electron affinity of the acceptor, as calculated at the G3X(MP2)-RAD(+) level of theory. R'^{+} SR^{-} refers to charge transfer from the alkyl fragment to the thiyl fragment, while R'^{-} SR^{+} refers to charge transfer from the thiyl to the alkyl fragment. NBO charges were obtained from the MPW1K/6-311+G(3df,2p) wave function, calculated with use of the MPW1K/6-31+G(d,p) optimized geometries. [b] Transition structure number, as illustrated in Figure 3.

The (linear) correlation for the n samples was then deemed to be statistically significant at an α% level of significance if the following inequality was satisfied.[48]

$$\left|\frac{r\sqrt{n-2}}{\sqrt{1-r^2}}\right| \geq t_{\alpha/2,n-2} \qquad (5)$$

It is important to stress that this statistical analysis assumes that the errors in the calculated barriers, enthalpies, singlet−triplet gaps, charge-transfer energies, and charges are random, which is unlikely to be the case. Nonetheless, in the absence of more specific information on the error distribution in these variables, the above analysis should at least provide a reasonable indication of the statistical significance of any observed correlations.

Finally, it should be noted that the aim of this study is to understand the underlying influences on barrier heights in hydrogen abstraction reactions, rather than to predict actual reaction rates. For this reason, barriers were calculated at 0 K, and corrections for quantum-mechanical tunneling have not been included. Without these additional calculations, direct comparisons between the calculated 0 K barriers and experimental Arrhenius activation energies are not meaningful. Fortunately, however, such comparisons are not necessary for the present purposes. For the present analysis to be meaningful, it is only necessary that the level of theory be sufficiently accurate for the trends in the data to be quantitatively reproduced. In the present work, the barriers, enthalpies, and associated thermodynamic quantities have been calculated at a consistent level of theory, G3X(MP2)-RAD. The accuracy of this (high) level of theory has been established in previously published assessment studies of both hydrogen abstraction barriers[45] and the thermodynamic properties of free radicals.[47]

4. Results and Discussion

Barriers and enthalpies were calculated for hydrogen atom abstraction reactions of the form $RS-H + {}^{\bullet}R' \rightarrow RS^{\bullet} + H-R'$. We explored the effect of the thiol substituent (R = CH_3, CH_2Cl, $CHCl_2$, CCl_3 CH_2F, CH_2OH, CH_2SH, CH_2CN, CH_2CH_3, $CH_2CH_2CH_3$, CH_2Ph, $CH_2C(CH_3)_3$) in reactions with the methyl radical (R′ = CH_3) (see Table 1), and the effect of the alkyl radical substituent (R′ = CH_3, CH_2Cl, $CHCl_2$, CCl_3 CH_2F, CH_2OH, CH_2SH, CH_2CN, CH_2CH_3, $CH_2CH_2CH_3$, CH_2Ph, $CH_2C(CH_3)_3$) in reactions with CH_3SH (see Table 2). We also examined reactions involving various combinations of the substituted alkyl radicals with the substituted thiols (see Table 3). Schematic diagrams showing the main features of the transition structures for the reactions in Tables 1−3 are provided in Figures 3−5, respectively; complete geometries of all species are provided in the Supporting Information.

The aim of the present work is to identify the principal factors influencing the barrier heights of the hydrogen abstraction reactions. To assist in the analysis, the natural bond orbital (NBO) charges on the alkyl and thiyl fragments in the transition structures and the energies for charge transfer between the isolated alkyl and thiyl radicals have also been calculated, and are included in Tables 1−3. The charge-transfer energies were obtained as the difference of the vertical ionization energy (IE) of the donor species and the vertical electron affinity (EA) of the acceptor species, and the individual IE and EA values of the alkyl and thiyl radicals are shown in Table 4. The vertical singlet−triplet gaps of the corresponding alkanes and thiols, together with their R′−H and RS−H bond dissociation energies (BDEs), are also included in Table 4. In what follows, we use these quantities in conjunction with the curve-crossing model[31−33] to provide a qualitative rationalization of the trends in reactivity in hydrogen abstraction from thiols by carbon-centered radicals. Before proceeding to the analysis of the barrier heights, we begin with a brief examination of the reaction enthalpies.

Reaction Enthalpies. From Tables 1−3, it is clear that hydrogen abstraction by carbon-centered radicals from thiols is generally an exothermic process, in which a strong C−H bond is formed at the expense of the weaker S−H bond. This is in accord with previous studies of biologically relevant systems,[49] and is consistent with the idea that hydrogen transfer from a thiol to a carbon-centered radical could help to limit oxidative damage in proteins. Nonetheless, the exothermicities are affected by the substituents on the alkyl radical and, to a lesser extent, the thiol. For example, the substituents in the present work cause variations in the exothermicities of approximately 10 kJ mol^{-1} in the reactions of the substituted thiols with $^{\bullet}CH_3$ (Table 1), and over 65 kJ mol^{-1} in the reactions of the substituted alkyl radicals with $HSCH_3$ (Table 2). The reaction of the stable alkyl radical $^{\bullet}CH_2Ph$ with $HSCH_3$ is only weakly exothermic, and it is thus conceivable that abstraction from alkanes by thiyl radicals

TABLE 2: Forward Barrier ($\Delta H^{\ddagger}_{fwd}$), Reverse Barrier ($\Delta H^{\ddagger}_{rev}$), Enthalpy ($\Delta H$), Charge-Transfer Energies (R'^{+} SR^{-} and R'^{-} SR^{+}), and NBO Charges (Q) on the Alkyl and Thiyl Fragments in the Transition Structures for $^{\bullet}R' + H-SCH_3 \rightarrow R'-H + {}^{\bullet}SCH_3$[a]

$^{\bullet}R'$	TS[b]	$\Delta H^{\ddagger}_{fwd}$	$\Delta H^{\ddagger}_{rev}$	ΔH	R'^{+} SR^{-}	R'^{-} SR^{+}	Q(alkyl)	Q(thiyl)
$^{\bullet}CH_3$	*1*	17.2	90.1	−72.8	7.97	10.69	0.008	−0.123
$^{\bullet}CCl_3$	*14*	14.2	43.6	−29.3	6.65	9.69	−0.077	−0.057
$^{\bullet}CHCl_2$	*15*	17.6	56.4	−38.9	6.70	10.15	−0.042	−0.085
$^{\bullet}CH_2Cl$	*16*	19.7	70.4	−50.8	6.96	10.52	−0.013	−0.105
$^{\bullet}CH_2F$	*17*	18.1	77.4	−59.3	7.65	11.03	0.029	−0.117
$^{\bullet}CH_2OH$	*18*	16.4	55.9	−39.6	6.15	11.53	0.062	−0.165
$^{\bullet}CH_2SH$	*19*	21.3	54.8	−33.5	5.70	10.87	0.013	−0.147
$^{\bullet}CH_2CN$	*20*	27.8	67.4	−39.7	8.44	9.06	−0.075	−0.046
$^{\bullet}CH_2CH_3$	*21*	11.2	69.5	−58.3	6.75	11.06	0.017	−0.140
$^{\bullet}CH_2CF_3$	*22*	10.7	90.6	−79.9	8.96	9.60	−0.038	−0.068
$^{\bullet}CH_2CH_2CH_3$	*23*	7.7	67.5	−59.9	6.61	10.87	0.018	−0.143
$^{\bullet}CH_2Ph$	*24*	31.0	43.4	−12.4	5.46	9.78	−0.011	−0.129
$^{\bullet}CH_2$(*t*-Bu)	*25*	2.1	66.9	−64.8	6.42	10.59	0.013	−0.141

[a] Barriers and enthalpies (0 K, kJ mol^{-1}) were calculated at the G3X(MP2)-RAD level of theory and include MPW1K/6-31+G(d,p) scaled zero-point vibrational energy. Charge-transfer energies (eV) were calculated as the difference in the vertical ionization energy of the donor species and the vertical electron affinity of the acceptor, as calculated at the G3X(MP2)-RAD(+) level of theory. R'^{+} SR^{-} refers to charge transfer from the alkyl fragment to the thiyl fragment, while R'^{-} SR^{+} refers to charge transfer from the thiyl to the alkyl fragment. NBO charges were obtained from the MPW1K/6-311+G(3df,2p) wave function, calculated with use of the MPW1K/6-31+G(d,p) optimized geometries. [b] Transition structure number, as illustrated in Figure 4.

TABLE 3: Forward Barrier ($\Delta H^{\ddagger}_{fwd}$), Reverse Barrier ($\Delta H^{\ddagger}_{rev}$), Enthalpy ($\Delta H$), Charge-Transfer Energies (R'^{+} SR^{-} and R'^{-} SR^{+}), and Charges (Q) on the Alkyl and Thiyl Fragments in the Transition Structures for $^{\bullet}R' + H-SR \rightarrow R'-H + {}^{\bullet}SR$[a]

$^{\bullet}R'$	H−SR	TS[b]	$\Delta H^{\ddagger}_{fwd}$	$\Delta H^{\ddagger}_{rev}$	ΔH	R'^{+} SR^{-}	R'^{-} SR^{+}	Q(alkyl)	Q(thiyl)
$^{\bullet}CH_2Cl$	$H-SCH_2(Cl)$	*26*	12.5	60.6	−48.1	6.30	10.78	0.008	−0.131
$^{\bullet}CH_2Cl$	$H-SCH_2(OH)$	*27*	15.6	64.2	−48.6	6.62		0.003	−0.127
$^{\bullet}CH_2Cl$	$H-SCH_2(CN)$	*28*	11.0	56.3	−45.3	6.07	11.28	0.021	−0.147
$^{\bullet}CH_2Cl$	$H-SCH_2(CH_3)$	*29*	17.0	66.5	−49.5	6.86	10.33	−0.016	−0.102
$^{\bullet}CH_2Cl$	$H-SCH_2(CF_3)$	*30*	12.5	54.8	−42.3	6.30	11.22	0.011	−0.138
$^{\bullet}CH_2Cl$	$H-SCH_2$(*t*-Bu)	*31*	13.6	59.0	−45.4	6.74	10.15	−0.011	−0.112
$^{\bullet}CH_2OH$	$H-SCH_2(Cl)$	*32*	−0.9	36.1	−36.9	5.49	11.79	0.088	−0.201
$^{\bullet}CH_2OH$	$H-SCH_2(OH)$	*33*	−2.2	35.2	−37.4	5.81		0.074	−0.189
$^{\bullet}CH_2OH$	$H-SCH_2(CN)$	*34*	−9.3	24.8	−34.1	5.26	12.29	0.110	−0.229
$^{\bullet}CH_2OH$	$H-SCH_2(CH_3)$	*35*	15.7	53.9	−38.3	6.05	11.35	0.060	−0.163
$^{\bullet}CH_2OH$	$H-SCH_2(CF_3)$	*36*	2.8	33.9	−31.1	5.49	12.23	0.090	−0.204
$^{\bullet}CH_2OH$	$H-SCH_2$(*t*-Bu)	*37*	10.1	44.3	−34.2	5.93	11.17	0.065	−0.175
$^{\bullet}CH_2CN$	$H-SCH_2(Cl)$	*38*	23.5	60.6	−37.0	7.79	9.33	−0.056	−0.070
$^{\bullet}CH_2CN$	$H-SCH_2(OH)$	*39*	27.0	64.5	−37.5	8.10		−0.059	−0.069
$^{\bullet}CH_2CN$	$H-SCH_2(CN)$	*40*	23.6	57.8	−34.2	7.56	9.83	−0.042	−0.086
$^{\bullet}CH_2CN$	$H-SCH_2(CH_3)$	*41*	24.9	63.3	−38.4	8.35	8.88	−0.080	−0.042
$^{\bullet}CH_2CN$	$H-SCH_2(CF_3)$	*42*	23.5	54.7	−31.2	7.79	9.77	−0.052	−0.077
$^{\bullet}CH_2CH_3$	$H-SCH_2(Cl)$	*43*	3.0	58.7	−55.7	6.10	11.32	0.036	−0.165
$^{\bullet}CH_2CH_3$	$H-SCH_2(OH)$	*44*	6.6	62.8	−56.2	6.41		0.030	−0.158
$^{\bullet}CH_2CH_3$	$H-SCH_2(CN)$	*45*	2.1	54.9	−52.8	5.87	11.82	0.048	−0.179
$^{\bullet}CH_2CH_3$	$H-SCH_2(CH_3)$	*46*	10.0	67.1	−57.0	6.66	10.87	0.015	−0.137
$^{\bullet}CH_2CH_3$	$H-SCH_2(CF_3)$	*47*	3.8	53.7	−49.9	6.10	11.76	0.039	−0.171
$^{\bullet}CH_2CH_3$	$H-SCH_2$(*t*-Bu)	*48*	7.1	60.1	−53.0	6.54	10.69	0.020	−0.147
$^{\bullet}CH_2$(*t*-Bu)	$H-SCH_2(Cl)$	*49*	−5.1	57.1	−62.2	5.76	10.85	0.032	−0.165
$^{\bullet}CH_2$(*t*-Bu)	$H-SCH_2(CH_3)$	*50*	0.6	64.1	−63.5	6.33	10.41	0.011	−0.139

[a] Barriers and enthalpies (0 K, kJ mol^{-1}) were calculated at the G3X(MP2)-RAD level of theory and include MPW1K/6-31+G(d,p) scaled zero-point vibrational energy. Charge-transfer energies (eV) were calculated as the difference in the vertical ionization energy of the donor species and the vertical electron affinity of the acceptor, as calculated at the G3X(MP2)-RAD(+) level of theory. R'^{+} SR^{-} refers to charge transfer from the alkyl fragment to the thiyl fragment, while R'^{-} SR^{+} refers to charge transfer from the thiyl to the alkyl fragment. NBO charges were obtained from the MPW1K/6-311+G(3df,2p) wave function, calculated with use of the MPW1K/6-31+G(d,p) optimized geometries. [b] Transition structure number, as illustrated in Figure 5.

could be thermodynamically preferred for appropriately substituted systems. Indeed, on the basis of the S−H BDEs in Table 4, one would predict that H-abstraction by the $CF_3CH_2S^{\bullet}$ radical from H−R would be exothermic when R is a strong radical stabilizing substituent such as $CH_2CH{=}CH_2$ (the previously reported[50] R−H BDE in this case being 355.7 kJ mol^{-1} at the G3(MP2)-RAD level of theory).

As noted above, the effect of the thiol substituent on the reaction enthalpy is much smaller than that of the alkyl substituent. This is reinforced in Table 4, where it is seen that the S−H BDEs of the thiols fall into a relatively narrow range despite the wide variation in the properties of the substituents. By contrast, the same substituents exert substantial effects on the corresponding C−H BDEs of the alkanes. This reduced sensitivity of thiols to substituent effects can be explained in terms of the location of the substituent. In the case of the alkanes, the substituent is attached directly to the hydrogen of the C−H bond, and bears the unpaired electron in the corresponding alkyl radical. In contrast, the substituents are removed from the hydrogen atom of the S−H bond in the thiols (and from the unpaired electron in the corresponding thiyl radical) by the intervening sulfur atom. This to some extent insulates the substituent from the breaking S−H bond, thereby reducing its effect on the S−H bond dissociation energy.

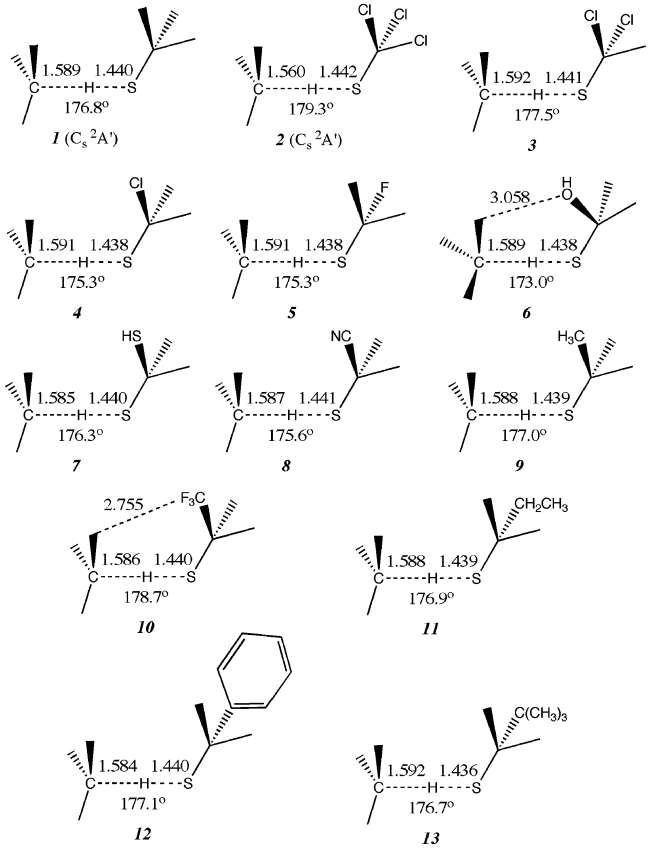

Figure 3. Schematic diagrams showing the principal geometric parameters in the MPW1K/6-31+G(d,p) optimized transition structures for the reaction of $^{\bullet}CH_3$ with various thiols (H−SR; R = CH_3, CH_2Cl, $CHCl_2$, CCl_3 CH_2F, CH_2OH, CH_2SH, CH_2CN, CH_2CH_3, $CH_2CH_2CH_3$, CH_2Ph, $CH_2C(CH_3)_3$).

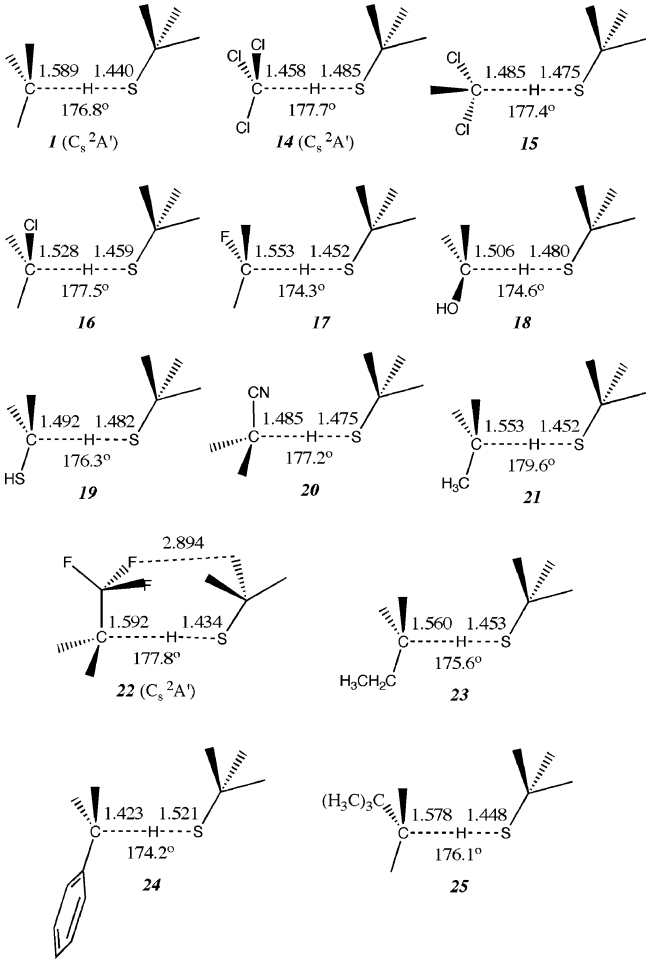

Figure 4. Schematic diagrams showing the principal geometric parameters in the MPW1K/6-31+G(d,p) optimized transition structures for the reaction of H−SCH_3 with various alkyl radicals ($^{\bullet}R'$; R′ = CH_3, CH_2Cl, $CHCl_2$, CCl_3 CH_2F, CH_2OH, CH_2SH, CH_2CN, CH_2CH_3, $CH_2CH_2CH_3$, CH_2Ph, $CH_2C(CH_3)_3$).

Reaction Barriers. As outlined above, the curve-crossing model predicts that the barrier height in the hydrogen abstraction reactions is influenced by the reaction exothermicity, the DA−DA[3] separation in the reactants or products (measured using the singlet−triplet gaps or bond dissociation energies of the closed-shell substrates), and the relative energies of the D^+A^- and D^-A^+ charge-transfer configurations, if these are sufficiently low in energy to contribute to the ground-state wave function. To explore the effect of each of these quantities on the hydrogen abstraction barriers, we have plotted the reaction barriers against (a) the reaction enthalpy, (b) the average singlet−triplet gap of the closed-shell reactants and products, (c) the energy for charge transfer between the isolated alkyl and thiyl fragments, and (d) the difference in the charges on the alkyl and thiyl fragments of the transition structures (see Figure 6). The corresponding correlation coefficients for the individual series in parts a−d of Figure 6, as well as those for the overall data sets in each case, are provided in Table 5.

Examining Figure 6a, we see that there is no apparent correlation between the barrier height and the reaction enthalpy, and hence the Evans−Polanyi rule[51] does not hold for these reactions. This is confirmed in Table 5, where it is seen that the correlation coefficient for the collected data is low, and is not statistically significant—even at the 10% level. When the reactions of a specific radical with a series of thiols are examined, the correlation is better, particularly for the less electron-donating radicals. However, in stark contrast to the Evans−Polanyi rule, the correlations are negative. That is, the barrier decreases as the reaction enthalpy increases (i.e. as the reactions become *less* exothermic). This unusual behavior can be understood when it is noted that, within a series, the enthalpy is itself weakly correlated with the electron affinity of the product thiyl species (for example, the correlation coefficient is 0.680 for the $^{\bullet}CH_3$ series). At least over the substituents considered in the present work, the enthalpy within a series generally increases as the electron affinity of the RS$^{\bullet}$ thiyl increases, and this probably reflects a strengthening of the RS−H bond of the reactant thiol through its increasing ionic character. As will be seen below, the barrier height decreases with the relative energy of the R'^+ SR^- configuration (and hence with the increasing electron affinity of the thiyl species), due to the stabilizing influence of polar interactions in the transition structures. It thus seems that the barrier-lowering influence of the increasing electron affinity of the thiyl dominates the barrier-raising influence of the concurrently increasing reaction enthalpy, leading to the negative correlation coefficient. Interestingly, the correlation coefficient for the combined data set, though very low, is at least positive. Once the reactions of *different* alkyl radicals are considered together, the correlation between the strength of the polar interactions in the transition structures and the enthalpy breaks down, and the (previously obscured) barrier-raising influence of the increasing reaction enthalpy becomes more evident, though the correlation remains poor due to the interference of the polar interactions.

Turning our attention to the singlet−triplet gaps of the substrates (Figure 6b), we note that there is also no apparent

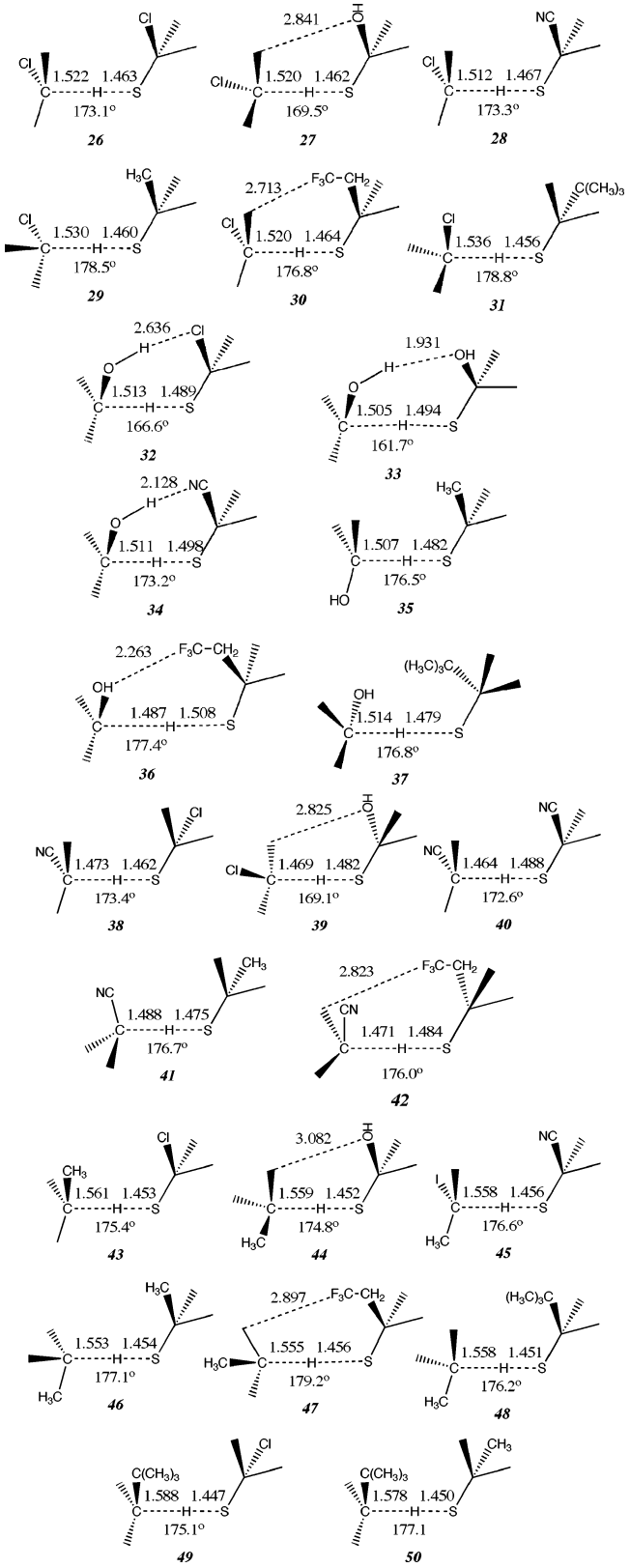

Figure 5. Schematic diagrams showing the principal geometric parameters in the MPW1K/6-31+G(d,p) optimized transition structures for the reaction of substituted thiols (H−SR) with various substituted alkyl radicals ($^{\bullet}$R′,R′ = CH_3, CH_2Cl, $CHCl_2$, CCl_3 CH_2F, CH_2OH, CH_2SH, CH_2CN, CH_2CH_3, $CH_2CH_2CH_3$, CH_2Ph, $CH_2C(CH_3)_3$).

correlation between this quantity and the barrier height. This is confirmed in Table 5, where it is seen that the respective correlation coefficients—both for reactions of specific radicals with a series of thiols, and for the combined data set—are not significant, even at the 10% level. This is in stark contrast to previous studies of other classes of hydrogen abstraction reactions,[9,10] in which it was concluded that the singlet−triplet gap was the dominant influence on the barrier heights. Two factors may help to explain the lack of correlation in the present systems. First, the relatively minor influence of the singlet−triplet gaps may be related to the early transition structures in these reactions, which are characterized by relatively long C−H forming bonds and relatively short breaking S−H bonds. As a result of this, the transition structure is dominated by the DA−DA[3] gap in the reactant-like geometries (i.e. thiols), rather than the product-like geometries (i.e. alkanes). As noted above, unlike the alkanes, the singlet−triplet gaps (and associated bond dissociation energies) of the thiols are relatively unaffected by the nature of the substituents, and fall into a relatively narrow range for the reactions considered in the present work. This can be seen quite clearly in Figure 6b, where the average singlet−triplet gap depends almost entirely on the attacking radical (or more specifically, the singlet−triplet of the alkane product) rather than the substituents on the thiol. The only exception to this is the series of reactions with the $^{\bullet}CH_3$ radical, for which a wider range of thiols was considered. It is perhaps significant that this series has the strongest (albeit weak) positive correlation between the barrier height and the singlet−triplet gap.

The second factor distinguishing the present systems from those of previous studies[9,10] is the dominant influence of polar interactions. This is seen quite clearly in Figure 6, parts c and d, in which there is a reasonable correlation between the barrier height and the charge-transfer energies (Figure 6c) and the degree of charge separation in the transition structure (Figure 6d). This is confirmed quantitatively in Table 5, in which it is seen that the corresponding correlation coefficients are large and statistically significant at the 5% level. In general, the barrier for hydrogen abstraction decreases as the charge-transfer energy *decreases* (positive correlation), reflecting the increasing ability of the charge-transfer configurations to stabilize the transition structure. Concurrently, the barrier decreases as the charge separation *increases* (negative correlation)—again reflecting the increasing degree of charge-transfer stabilization of the transition structures. In all cases the preferred direction of charge transfer is from the alkyl radical to the thiyl radical (i.e. the R'^{+} SR^{-} configuration is preferred). This is evident in both the lower charge-transfer energies for the R'^{+} SR^{-} configurations (compared to the R'^{-} SR^{+} configurations) in the isolated reactants, and also the significant negative charges borne by the thiyl fragments in the transition structures (see Tables 1−3). As a result of this, the reaction barriers are generally the lowest for the most nucleophilic radicals (such as $^{\bullet}CH_2OH$), and highest for the most electrophilic alkyl radicals (such as $^{\bullet}CH_2CN$). Indeed, the reduced importance of polar interactions in this latter case can help to explain the poorer correlation between the barrier height and the charge-transfer energies, and between the barrier height and the degree of charge separation, within this series.

The present results thus suggest that polar interactions are the predominant influence on barrier heights in hydrogen abstraction from thiols by carbon-centered radicals, and this is in accord with the conclusions of previous studies of related reactions.[2,25−30] However, a closer examination of the data reveals that other factors also play a role. For example, the reactions involving the $^{\bullet}CH_2C(CH_3)_3$ radical have lower reaction barriers than those with the $^{\bullet}CH_3$ and $^{\bullet}CH_2CH_3$ radicals, despite the similar level of charge separation. This might reflect the smaller singlet−triplet gaps in the former case. The $^{\bullet}CH_2OH$

TABLE 4: Vertical Ionization Energies (IEs) and Electron Affinities (EAs) of the Alkyl and Thiyl Radicals, and Vertical Singlet−Triplet (S−T) Gaps and Bond Dissociation Energies (BDEs) of the Corresponding Alkanes and Thiols[a]

	IE (eV)		EA (eV)		S−T gap (eV)		BDE (kJ mol^{-1})	
R	R$^\bullet$	RS$^\bullet$	R$^\bullet$	RS$^\bullet$	RH	RSH	R−H	RS−H
CH_3	9.83	10.57	−0.12	1.85	10.27	5.17	429.7	356.9
CCl_3	8.51	10.83	0.88	3.15	6.21	4.69	386.2	363.2
$CHCl_2$	8.56	10.81	0.42	2.92	7.74	4.90	395.7	363.7
CH_2Cl	8.81	10.83	0.05	2.51	6.35	5.20	407.6	359.5
CH_2F	9.50	11.10	−0.46	2.30	9.52	5.56	416.1	356.2
CH_2OH	8.00		−0.96	2.20	6.76	5.39	396.4	359.0
CH_2SH	7.56	9.30	−0.30	2.19	5.17	4.79	390.3	357.5
CH_2CN	10.30	11.33	1.51	2.74	7.33	5.14	396.5	362.4
CH_2CH_3	8.61	10.39	−0.49	1.95	10.45	5.19	415.2	358.2
CH_2CF_3	10.82	11.27	0.98	2.51	10.99	5.43	436.8	365.3
$CH_2CH_2CH_3$	8.46	10.32	−0.30	1.96	8.51	5.21	416.7	358.4
CH_2Ph	7.31	8.90	0.79	2.17	4.56	4.39	369.2	360.4
CH_2(*t*-Bu)	8.27	10.21	−0.02	2.07	8.24	5.33	421.7	362.2

[a] Vertical ionization energies, electron affinities, and singlet−triplet gaps (0 K, eV) were calculated at the G3X(MP2)-RAD(+)//MPW1K/6-31+G(d,p) level of theory. Bond dissociation energies (0 K, kJ mol^{-1}) were calculated at the G3X(MP2)-RAD level of theory, and include MPW1K/6-31+G(d,p) scaled zero-point vibrational energy.

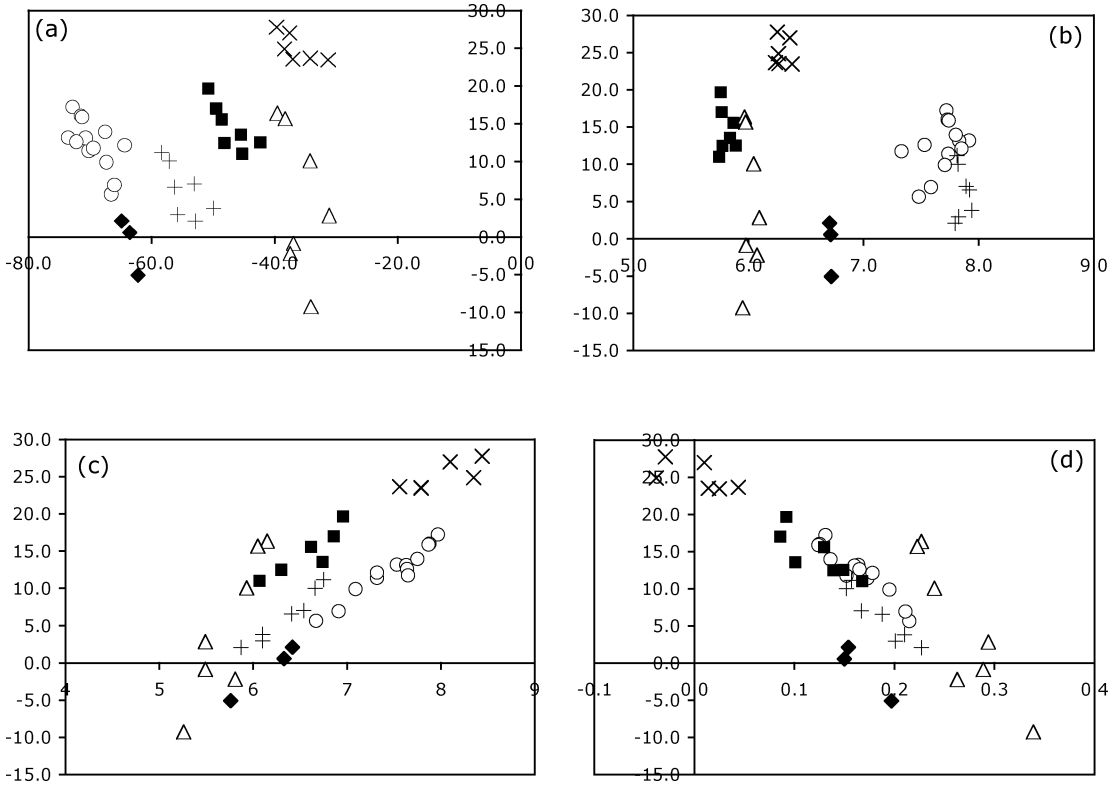

Figure 6. Plots of the reaction barrier (kJ mol^{-1}) versus (a) reaction enthalpy (kJ mol^{-1}), (b) average singlet−triplet gap (eV) of the closed shell reactants and products, (c) the energy for charge transfer (eV) between isolated alkyl and thiyl fragments, and (d) difference in the charges on the alkyl and thiyl fragments in the transition structures. Each series shows the reactions of various substituted thiols with a specific alkyl radical: ○ = $^\bullet CH_3$; × = $^\bullet CH_2CN$; △ = $^\bullet CH_2OH$; ■ = $^\bullet CH_2Cl$; + = $^\bullet CH_2CH_3$; ♦ = $CH_2C(CH_3)_3$.

series, while showing a reasonable correlation between barrier height and charge separation, has a different slope to the other series. This may in part be the result of additional stabilizing interactions in the transition structures for the reactions with the four lowest barriers. It can be seen in Figure 5 that, in those four transition structures (*32*, *33*, *34*, and *36*), the oxygen of the $^\bullet CH_2OH$ radical lies within 3 Å or less of a hydrogen atom in the thiol, and hence H-bonding may be occurring. Indeed, for three of these reactions, the barriers are actually slightly negative—implying that some form of weakly bound precomplex is formed prior to the reaction. The other $^\bullet CH_2OH$ reactions have higher barriers when compared with the reactions of radicals having similar degrees of charge separation in their transition structures, and this may reflect the larger reaction enthalpies in the former case.

The complexity of the trends in reactivity is further highlighted when the reactions of a wider range of alkyl radicals are examined. Figure 7 shows the barrier heights versus the charge separation for reactions of various alkyl radicals with $HSCH_3$. For the sake of comparison, this plot is superimposed on the data for the reactions of specific alkyl radicals with substituted thiols, as plotted in Figure 6d. It can be seen that the correlation between the barrier height and the charge separation is poor for the $HSCH_3$ series. In fact if we examine the correlation coefficients in Table 5, we find that there is no statistically significant correlation between barrier height and

TABLE 5: Coefficients of Correlation between the Barrier Height and the Reaction Enthalpy (ΔH), the Average Singlet−Triplet Gap of the Reactant Thiol and Product Alkane (S−T Gap), the Relative Energy of the R'^{+} SR^{-} Configuration (R'^{+} SR^{-}), and the Charge Difference between the Alkyl and Thiyl Fragments in the Transition Structures of the Hydrogen Abstraction Reactions (ΔQ)[a]

	correlation coefficient					|test statistic|				$t_{\alpha/2,n-2}$	
series[b]	ΔH	S−T gap	R'^{+} SR^{-}	ΔQ	n	ΔH	S−T gap	R'^{+} SR^{-}	ΔQ	5% level	10% level
$^{\bullet}CH_3$	−0.661	0.446	0.966	−0.953	13	2.922	1.653	12.406	10.401	2.201	1.796
$^{\bullet}CH_2CN$	−0.714	0.017	0.792	−0.589	6	2.042	0.035	2.596	1.459	2.776	2.132
$^{\bullet}CH_2OH$	−0.461	−0.095	0.897	−0.917	7	1.161	0.214	4.546	5.131	2.571	2.015
$^{\bullet}CH_2Cl$	−0.788	−0.171	0.907	−0.823	7	2.865	0.389	4.812	3.242	2.571	2.015
$^{\bullet}CH_2CH_3$	−0.686	−0.134	0.977	−0.948	7	2.107	0.302	10.148	6.627	2.571	2.015
all in Figure 6	0.136	−0.158	0.796	−0.848	43	0.879	1.023	8.427	10.230	2.020	1.683
$HSCH_3$	0.670	−0.557	−0.087	−0.256	13	2.990	2.225	0.288	0.879	2.201	1.796
all in Figure 7	0.274	−0.275	0.553	−0.754	50	1.977	1.981	4.596	7.962	2.013	1.679

[a] The correlation coefficient (r) for the n samples is deemed to be significant at α% level if the absolute value of the corresponding test statistic ($r(n-2)^{0.5}/(1-r^2)^{0.5}$) exceeds the corresponding $t_{\alpha/2,n-2}$ value (see text). [b] See Figures 6a−d and 7.

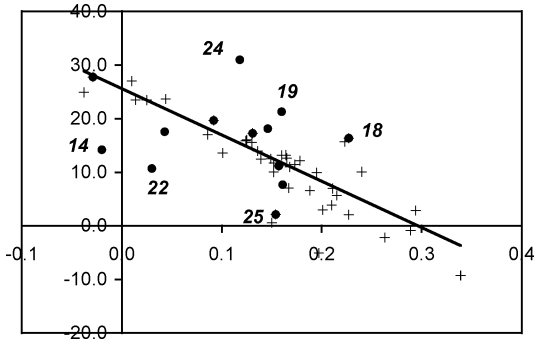

Figure 7. Plots of the reaction barrier (kJ mol^{-1}) versus the difference in the charges on the alkyl and thiyl fragments in the transition structures. The reactions of the various alkyl radicals with $HSCH_3$ are marked with a ● symbol, while the reactions with the other thiols are marked with a + symbol. The numbers refer to transition structures in Figure 4.

charge-transfer energy or charge separation for the series, though a statistically significant correlation remains for the combined data set.

The lack of correlation between charge separation and barrier height in the $HSCH_3$ series probably reflects (at least in part) the wider range of singlet−triplet gaps and reaction enthalpies covered by the additional alkyl radicals. Indeed, within this series, the correlations between the barrier heights and the singlet−triplet gaps, and between the barrier heights and the reaction enthalpies, are both statistically significant (see Table 5). In the case of the enthalpies, the correlation is positive, as would be expected under the Evans−Polanyi rule. Thus, for example, the reaction of the $^{\bullet}CH_2Ph$ radical (transition structure *24*) has a considerably higher barrier than the other reactions with similar degrees of charge separation in their transition structures, because it is considerably less exothermic. However, in the case of the singlet−triplet gaps, the correlation is negative—that is, the barrier height decreases as the average singlet−triplet increases, contrary to the predictions of the curve-crossing model. To explain this unusual behavior, it is first noted that the variation in the average singlet−triplet gap reflects the variation in the singlet−triplet gap of the alkane product (the thiol being constant within this series). Furthermore, the singlet−triplet gap of the alkane product is expected to increase with the strength of the forming C−H bond, and there is thus a strong negative correlation ($r = -0.894$) between the average singlet−triplet gap and the reaction enthalpy. As a result, within this series, the barrier increases as the singlet−triplet gap decreases, due to the concurrently increasing reaction enthalpy. This again illustrates the complex interactions between the factors influencing barrier heights in these hydrogen abstraction reactions.

Practical Aspects. Barrier heights in hydrogen abstraction from thiols are thus predominantly influenced by polar interactions (as measured using the charge-transfer energies of the isolated reactants or the degree of charge separation in the transition structures), but the influence of other quantities (such as the reaction exothermicity, the singlet−triplet gaps of the substrates, and direct interactions in the transition structures) obscures a direct predictive relationship. Although the focus of this study has been to apply a *qualitative* treatment of the curve-crossing model to the problem of rationalizing the trends in the hydrogen abstraction barriers, it is worth considering whether a *quantitative* treatment is possible. If successful, this would allow us to model the simultaneous effect of the various factors on the barrier height, and thereby derive some useful predictive formula for calculating the barrier heights in these reactions in terms of simple and easily accessible quantities.

Using the curve-crossing model, Song et al.[10] have derived various formulas for predicting the barrier height in nonidentity reactions, including the following compact expression:

$$\Delta H^{\ddagger} = f_a G_a + 0.5\Delta H - B \qquad (6)$$

In this equation G_a and f_a are the average G and f parameters for the forward and reverse reactions, with G measuring the DA−DA[3] promotion gap, and f the fraction of this promotion gap required to reproduce the height of the crossing point. The parameter B is the resonance energy at the crossing point, which, in the present reactions, will include contributions from both the resonance between the DA and DA[3] configurations, and also the resonance between these covalent configurations and the charge-transfer configurations. The f, G, and B parameters are directly accessible from quantitative valence bond theory calculations of the reactants and transition structures, but not the molecular orbital theory calculations of the present work. However, to render the formula more widely applicable, Song et al.[10] showed that the promotion gap is linearly related to the singlet−triplet excitation gap of the closed shell substrates, and (in the absence of polar interactions) the B parameter can be approximated as half of the bond dissociation energy of the originally weak bond (in this case the thiol). They also noted that the f_a parameter was relatively constant within a series of reactions.

To take into account the additional influence of polar interactions in the hydrogen abstraction reactions of the present work, eq 6 was extended as follows

$$\Delta H^{\ddagger} = c_1(S-T) + 0.5\Delta H - 0.5(\mathrm{BDE}) + c_2(R'^{+}RS^{\pm}) \qquad (7)$$

where $S - T$ is the average singlet triplet gap (eV) of the reactant

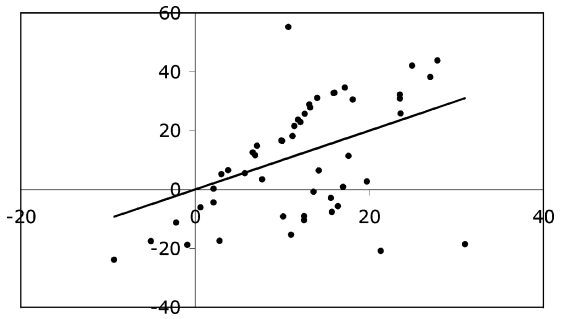

Figure 8. Plots of the fitted reaction barrier (kJ mol^{-1}), obtained from a least-squares fit to eq 7, versus the actual reaction barrier (kJ mol^{-1}). The solid line shows the hypothetical perfect fit.

thiol and product alkane, ΔH is the reaction enthalpy (kJ mol^{-1}), BDE is the bond dissociation energy (kJ mol^{-1}) of the *thiol*, and R'^{+} SR^{-} is the relative energy (eV) of the R'^{+} SR^{-} charge-transfer configuration. The term $c_2(R'^{+}\ SR^{-})$ represents the additional covalent-ionic contribution to *B*, the covalent contribution being modeled as 0.5(BDE), as in eq 6. The use of a linear relationship between the charge-transfer energy and the resonance energy at the transition structure was motivated by the reasonable linear correlations between the charge-transfer energy and the barrier height that were observed for the reactions of the present work (see Figure 6c and Table 5). The proportionality constants $c_1 = 11.442$ and $c_2 = 20.216$ were estimated by fitting eq 7 to the set of 50 reaction barriers in the present work via linear regression. The c_1 parameter incorporates the f_a term of eq 6, the proportionality constant between the calculated singlet−triplet gap and the promotion gap (*G*), and the conversion factor from eV to kJ mol^{-1}. The c_2 parameter also incorporates this conversion factor, together with the proportionality constant between the resonance energy and charge-transfer energy.

It was found that the fit of eq 7 to the reaction barriers of the present work was extremely poor. This is illustrated in Figure 8, which shows the fitted barriers, plotted as a function of the actual reaction barriers. Although eq 7 assumed a linear relationship between the covalent-ionic resonance energy and the charge-transfer energy, variants of eq 7, in which the charge-transfer term was treated as an exponential or as a quadratic, also failed comprehensively to provide an adequate fit to the data. This failure is in contrast to the earlier study by Song et al.[10] in which eq 6 was extremely successful in reproducing the calculated barrier heights in the nonidentity reactions involving hydrogen transfer between Group IV hydrides. It seems that the influence of polar interactions on the trends in the barrier heights in the present systems, absent from the earlier study, complicates the quantitative curve-crossing analysis. The quantitative relationship between the initial charge-transfer energy and the barrier height is unlikely to be a simple analytical function, as it will depend not only on the change in the relative energies of the reactant, product, and charge-transfer configurations as the reactants approach each one another, but also on the resonance stabilization energy associated with the resulting degree of charge transfer. Additional complex inter-relationships between the individual terms of the crossing-model may also contribute to the failure of eq 7. For example, it was seen above that, in reactions of individual alkyl radicals with a series of thiols, the reaction enthalpy and the electron affinity of the thiyl fragment were correlated with one another. As a result, the barrier height decreased as the reaction enthalpy increased within a series, contrary to the predictions of the Evans−Polanyi rule and curve-crossing model. Moreover, when comparing the reactions of a specific thiol with a series of alkyl radicals, the singlet−triplet gap of the product alkane and the reaction enthalpy were correlated with one another. As a result, the barrier height decreased as the singlet−triplet gap increased within the series, contrary to the predictions of the curve-crossing model.

The curve-crossing model (at least in this simplified form) thus failed to allow for the quantitative prediction of barrier heights in the present hydrogen abstraction reactions, in terms of the properties of the isolated reactants. However, this does not diminish the value of the curve-crossing model for studying these systems. The quantitative prediction of barrier heights is not the main function of this model—this, after all, can be handled very effectively by quantum mechanics. Rather, the curve-crossing model helps to provide that which is lacking from a quantum-mechanical treatment, a qualitative understanding of the trends in barrier heights in terms of familiar chemical concepts. The qualitative analysis of the present work, though highlighting the complex nature of the reactions, still has some practical value. For example, the conclusion that polar interactions dominate the trends in the barrier heights allows one to predict qualitatively that, within a series of related reactions, barriers will generally be lower for abstraction by nucleophilic radicals (such as $^{\bullet}CH_2OH$) compared to electrophilic radicals (such as $^{\bullet}CH_2CN$). Barriers should also be lower when the thiols have relatively high electron affinities (such as $HSCCl_3$). Indeed, provided the reaction exothermicities are not too dissimilar, the qualitative ordering of barrier heights may be predicted on the basis of the charge-transfer energies of the isolated species. Such information may allow one, for example, to identify a small set of possible chain transfer agents for a particular polymerization system by selecting substituents that are expected to maximize the polar interactions, while maintaining a reasonably favorable exothermicity. Having identified suitable target compounds, the actual reaction barriers (and rates) could then be calculated quantitatively via ab initio molecular orbital calculations, so as to identify the most effective transfer agent for the particular system. The conclusion that polar interactions dominate the barrier heights in hydrogen abstraction from thiols by carbon-centered radicals also leads to the prediction that, in the solution phase, solvents having high dielectric constants will enhance the rates of these reactions. Hence it should be possible to exert some degree of practical control over the reaction rates in these systems through variation of the solvent.

5. Conclusions

Hydrogen abstraction by carbon-centered radicals from thiols is generally an exothermic process in which a strong C−H bond is formed at the expense of the weaker S−H bond of the thiol. The barrier heights are predominantly influenced by polar factors, with the reactions of nucleophilic radicals (such as $^{\bullet}CH_2OH$) being favored over reactions with electrophilic radicals (such as $^{\bullet}CH_2CN$). For the reactions of a specific alkyl radical with a series of substituted thiols, there is a reasonable correlation between the barrier height and the various measures of the importance of polar effects (such as the degree of charge separation in the transition structure or the energy for charge transfer between the isolated alkyl and thiyl fragments). When reactions of a wide range of alkyl radicals with a specific thiol are compared, the correlation is somewhat poorer and this reflects the influence of additional factors, such as the reaction exothermicity, the DA−DA[3] gap of the alkane product, and (in some cases) the additional stabilizing influence of direct H-bonding interactions in the transition structures.

Acknowledgment. We gratefully acknowledge generous allocations of computing time on the Compaq Alphaserver of the National Facility of the Australian Partnership for Advanced Computing and the Australian National University Supercomputing Facility, useful discussions with Professor Chris Easton, and provision of an Australian Research Council postdoctoral fellowship (to M.L.C.).

Supporting Information Available: Table S1 showing the MPW1K/6-31+G(d,p) optimized geometries,of the reactants, products and transition structures, in the form of GAUSSIAN archive entries. This material is available free of charge via the Internet at http://pubs.acs.org.

References and Notes

(1) See for example: Odian, G. *Principles of Polymerization*; Wiley-Interscience: New York, 1991.

(2) Cole, S. J.; Kirwan, J. N.; Roberts, B. P.; Willis, C. R. *J. Chem. Soc., Perkin Trans. 1* **1991**, 103−112.

(3) See for example: Wardman, P.; von Sonntag, C. *Methods Enzymol.* **1995**, *251*, 31−45.

(4) Zavitsas, A. A. *J. Am. Chem. Soc.* **1972**, *94*, 2779−2789.

(5) Zavitsas, A. A.; Melikian, A. A. *J. Am. Chem. Soc.* **1975**, *97*, 2757−2763.

(6) Zavitsas, A. A.; Chatgilialoglu, C. *J. Am. Chem. Soc.* **1995**, *117*, 10645−10654.

(7) Zavitsas, A. A. *J. Am. Chem. Soc.* **1998**, *120*, 6578−6586.

(8) Pross, A.; Yamataka, H.; Nagase, S. *J. Phys. Org. Chem.* **1991**, *4*, 135.

(9) (a) Shaik, S.; Wu, W.; Dong, K.; Song, L.; Hiberty, P. C. *J. Phys. Chem. A* **2001**, *105*, 8226. (b) Zavitsas, A. A. *J. Phys. Chem. A* **2002**, *106*, 5041. (c) Shaik, S.; de Visser, S. P.; Wu, W.; Song, L.; Hibberty, P. C. *J. Phys. Chem. A* **2002**, *106*, 5043.

(10) Song, L.; Wu, W.; Dong, K.; Hibberty, P. C.; Shaik, S. *J. Phys. Chem. A* **2002**, *106*, 11361−11370.

(11) Harcourt, R. D. *J. Phys. Chem. A* **2003**, *107*, 10324−10329.

(12) Salikhov, A.; Fischer, H. *Theor. Chim. Acc.* **1997**, *96*, 114−121.

(13) Yamataka, H.; Nagase, S. *J. Org. Chem.* **1988**, *53*, 3232.

(14) Fox, G. L.; Schlegel, H. B. *J. Phys. Chem.* **1992**, *96*, 298.

(15) Bernardi, F.; Bottoni, A. *J. Phys. Chem. A* **1997**, *101*, 1912.

(16) Pais, A. A. C. C.; Arnaut, L. G.; Formosinho, S. J. *J. Chem. Soc., Perkin Trans. 2* **1998**, 2577.

(17) Sumathi, R.; Carstensen, H. H.; Green, W. H., Jr. *J. Phys. Chem. A* **2001**, *105*, 6910−6925.

(18) Sumathi, R.; Carstensen, H. H.; Green, W. H., Jr. *J. Phys. Chem. A* **2001**, *105*, 8969−8984.

(19) (a) Roberts, B. P.; Steel, A. J. *J. Chem. Soc., Perkin Trans. 2* **1994**, 2155−2162. (b) Zavitsas, A. A. *J. Chem. Soc., Perkin Trans. 2* **1996**, 499−502. (c) Roberts, B. P. *J. Chem. Soc., Perkin Trans. 2* **1996**, 2719−2725. (d) Zavitsas, A. A. *J. Chem. Soc., Perkin Trans. 2* **1998**, 391−393.

(20) Ma, X.; Schobert, H. H. *Ind. Eng. Chem. Res.* **2001**, *40*, 743.

(21) Ma, X.; Schobert, H. H. *Ind. Eng. Chem. Res.* **2003**, *42*, 1151−1161.

(22) Pryor, W. A.; Fuller, D. L.; Stanley, J. P. *J. Am. Chem. Soc.* **1972**, *94*, 1632.

(23) Chandra, A. K.; Uchimaru, T.; Urata, S.; Sugie, M.; Sekiya, A. *Int. J. Chem. Kinet.* **2003**, *35*, 1305.

(24) Marcus, R. A. *J. Am. Chem. Soc.* **1969**, *91*, 7224−7225.

(25) Johnson, C. C.; Horner, J. H.; Tronche, C.; Newcomb, M. *J. Am. Chem. Soc.* **1995**, *117*, 1684−1687.

(26) Horner, J. H.; Martinez, F. N.; Musa, O. M.; Newcomb, M.; Shahin, H. E. *J. Am. Chem. Soc.* **1995**, *117*, 11124−11133.

(27) Dolbier, W. R., Jr.; Rong, X. X. *Tetrahedron Lett.* **1994**, *35*, 6225−6228.

(28) Rong, X. X.; Pan, H.-Q.; Dolbier, W. R., Jr. *J. Am. Chem. Soc.* **1994**, *116*, 4521−4522.

(29) Reid, D. L.; Shustov, G. V.; Armstrong, D. A.; Rauk, A.; Schuchmann, M. N.; Akhlaq, M. S.; von Sonntag, C. *Phys. Chem. Chem. Phys.* **2002**, *4*, 2965−2974.

(30) Reid, D. L.; Armstrong, D. A.; Rauk, A.; von Sonntag, C. *Phys. Chem. Chem. Phys.* **2003**, *5*, 3994−3999.

(31) Pross, A.; Shaik, S. S. *Acc. Chem. Res.* **1983**, *16*, 363.

(32) Pross, A. *Adv. Phys. Org. Chem.* **1985**, *21*, 99−196.

(33) Shaik, S. S. *Prog. Phys. Org. Chem.* **1985**, *15*, 197−337.

(34) See for example: Fischer, H.; Radom, L. *Angew. Chem., Int. Ed. Engl.* **2001**, *40*, 1340−1371 and references therein.

(35) Gómez-Balderas, R.; Coote, M. L.; Henry, D. J.; Fischer, H.; Radom, L. *J. Phys. Chem. A* **2003**, *107*, 6082−6090.

(36) Henry, D. J.; Coote, M. L.; Gómez-Balderas, R.; Radom, L. *J. Am. Chem. Soc.* **2004**, *126*, 1732−1740.

(37) Coote, M. L.; Pross, A.; Radom, L. In *Fundamental World of Quantum Chemistry*: *A Tribute to the Memory of Per-Olov Löwdin*; Brändas, E. J., Kryachko, E. J., Eds.; Kluwer-Springer: New York, 2004; Vol. III, in press.

(38) (a) Heitler, W.; London, F. *Z. Phys.* **1927**, *44*, 455. (b) Pauling, L. *The Nature of the Chemical Bond*; Cornell University Press: Ithaca, New York, 1939.

(39) (a) Woodward, R. B.; Hoffman, R. *Angew Chem.* **1969**, *81*, 797. (b) Woodward, R. B.; Hoffman, R. *Angew Chem., Int. Ed. Engl.* **1969**, *8*, 781.

(40) Hehre, W. J.; Radom, L.; Schleyer, P. v. R.; Pople, J. A. *Ab Initio Molecular Orbital Theory*; Wiley: New York, 1986.

(41) Koch, W.; Holthausen, M. C. *A Chemist's Guide to Density Functional Theory*; Wiley-VCH: Weinheim, Germany, 2000.

(42) Frisch, M. J.; Trucks, G. W.; Schlegel, H. B.; Scuseria, G. E.; Robb, M. A.; Cheeseman, J. R.; Zakrzewski, V. G.; Montgomery, J. A., Jr.; Stratmann, R. E.; Burant, J. C.; Dapprich, S.; Millam, J. M.; Daniels, A. D.; Kudin, K. N.; Strain, M. C.; Farkas, O.; Tomasi, J.; Barone, V.; Cossi, M.; Cammi, R.; Mennucci, B.; Pomelli, C.; Adamo, C.; Clifford, S.; Ochterski, J.; Petersson, G. A.; Ayala, P. Y.; Cui, Q.; Morokuma, K.; Malick, D. K.; Rabuck, A. D.; Raghavachari, K.; Foresman, J. B.; Cioslowski, J.; Ortiz, J. V.; Stefanov, B. B.; Liu, G.; Liashenko, A.; Piskorz, P.; Komaromi, I.; Gomperts, R.; Martin, R. L.; Fox, D. J.; Keith, T.; Al-Laham, M. A.; Peng, C. Y.; Nanayakkara, A.; Challacombe, M.; Gill, P. M. W.; Johnson, B.; Chen, W.; Wong, M. W.; Andres, J. L.; Gonzalez, C.; Head-Gordon, M.; Replogle, E. S.; Pople, J. A. *GAUSSIAN 98*; Gaussian, Inc.: Pittsburgh, PA, 1998.

(43) Frisch, M. J.; Trucks, G. W.; Schlegel, H. B.; Scuseria, G. E.; Robb, M. A.; Cheeseman, J. R.; Montgomery, J. A., Jr.; Vreven, T.; Kudin, K. N.; Burant, J. C.; Millam, J. M.; Iyengar, S. S.; Tomasi, J.; Barone, V.; Mennucci, B.; Cossi, M.; Scalmani, G.; Rega, N.; Petersson, G. A.; Nakatsuji, H.; Hada, M.; Ehara, M.; Toyota, K.; Fukuda, R.; Hasegawa, J.; Ishida, M.; Nakajima, T.; Honda, Y.; Kitao, O.; Nakai, H.; Klene, M.; Li, X.; Knox, J. E.; Hratchian, H. P.; Cross, J. B.; Adamo, C.; Jaramillo, J.; Gomperts, R.; Stratmann, R. E.; Yazyev, O.; Austin, A. J.; Cammi, R.; Pomelli, C.; Ochterski, J. W.; Ayala, P. Y.; Morokuma, K.; Voth, G. A.; Salvador, P.; Dannenberg, J. J.; Zakrzewski, V. G.; Dapprich, S.; Daniels, A. D.; Strain, M. C.; Farkas, O.; Malick, D. K.; Rabuck, A. D.; Raghavachari, K.; Foresman, J. B.; Ortiz, J. V.; Cui, Q.; Baboul, A. G.; Clifford, S.; Cioslowski, J.; Stefanov, B. B.; Liu, G.; Liashenko, A.; Piskorz, P.; Komaromi, I.; Martin, R. L.; Fox, D. J.; Keith, T.; Al-Laham, M. A.; Peng, C. Y.; Nanayakkara, A.; Challacombe, M.; Gill, P. M. W.; Johnson, B.; Chen, W.; Wong, M. W.; Gonzalez, C.; Pople, J. A. *Gaussian 03*, Revision B.03; Gaussian, Inc.: Pittsburgh, PA, 2003.

(44) Werner, H.-J.; Knowles, P. J.; Amos, R. D.; Bernhardsson, A.; Berning, A.; Celani, P.; Cooper, D. L.; Deegan, M. J. O.; Dobbyn, A. J.; Eckert, F.; Hampel, C.; Hetzer, G.; Korona, T.; Lindh, R.; Lloyd, A. W.; McNicholas, S. J.; Manby, F. R.; Meyer, W.; Mura, M. E.; Nicklass, A.; Palmieri, P.; Pitzer, R.; Rauhut, G.; Schütz, M.; Stoll, H.; Stone, A. J.; Tarroni, R.; Thorsteinsson, T. *MOLPRO*, 2000.6; University of Birmingham: Birmingham, 1999.

(45) Coote, M. L. *J. Phys. Chem. A* **2004**, *108*, 3865−3872.

(46) Lynch, B. J.; Truhlar, D. G. *J. Phys. Chem. A* **2001**, *105*, 2936−2941.

(47) Henry, D. J.; Sullivan, M. B.; Radom, L. *J. Chem. Phys.* **2003**, *118*, 4849−4860.

(48) Chatfield, C. *Statistics for Technology, A Course in Applied Statistics*, 3rd ed.; Chapman and Hall: London, UK, 1991.

(49) Rauk, A.; Yu, D.; Armstrong, D. A. *J. Am. Chem. Soc.* **1998**, *120*, 8848.

(50) Henry, D. J.; Parkinson, C. J.; Mayer, P. M.; Radom, L. *J. Phys. Chem. A* **2001**, *105*, 6750−6756.

(51) Evans, M. A.; Polanyi, M. *Trans. Faraday Soc.* **1938**, *34*, 11.